Green Chemistry

Cutting-edge research for a greener sustainable future

www.rsc.org/greenchem

Volume 12 | Number 7 | July 2010 | Pages 1113–1316

ISSN 1463-9262

RSC Publishing

Hydrogels formed through regulated self-organization of gradually charging chitosan in solution of xanthan†

Yury Shchipunov,*[a,b] Sergei Sarin,[a] Il Kim[b] and Chang-Sik Ha[b]

Received 30th November 2009, Accepted 11th May 2010
First published as an Advance Article on the web 4th June 2010
DOI: 10.1039/b925138c

Hydrogels are prepared by means of progressive acidification of xanthan solution containing dispersed chitosan particles in noncharged state at pH a little larger than pK_a of this polysaccharide. The following pH shift causes gradual charging of chitosan macromolecules that are involved into electrostatic interactions with oppositely charged xanthan. This triggered self-regulating processes of polysaccharide self-organization into supramolecular structures. Fibrillation or capsulation was observed that depended on the charge mixing ratio between chitosan and xanthan. The jellification of solutions took place in a case of fibrillar morphology. The strongest hydrogels were found where a fine and dense network of aligning fibrils of mean diameter of around 30 nm were generated. Where oppositely charged polysaccharides self-organized into capsules, the hydrogel was not formed because of the absence of cross-links between particles that could reach few mm in diameter and had mechanically strong shell.

1. Introduction

Chitosan is derived by de-acetylation of chitin, which is the second abundant organic compound on Earth after the cellulose.[1–3] Chitinous structures occur mainly in crustaceans, mollusks, insects and fungi. As estimated, as much as 100 billion tons of chitin are produced annually in living nature. It presents a huge renewal resource of biomass that is still almost unutilized. Numerous studies demonstrate that this polysaccharide possesses distinctive physico-chemical properties and biological activities including film- and fiber-forming, coating, metal-ion absorbing and coagulating properties, antiseptic, wound-healing and immune-stimulating activities, biocompatibility, bioresorbability and biodegradability.[3–12] The whole range of mentioned advantages is superior to that of cellulose. Therefore, the chitin and its derivative chitosan is believed to have much higher potential for applications in many fields, being an extraordinary underexploited biopolymer of significant versatility and promise.[2,3,10]

A severe restriction on chitosan use is caused by its incapability to form hydrogels.[6,13,14] To obviate the problem, numerous means are suggested. Their common feature is that they include chemical modification or chemical cross-linking of polysaccharide macromolecules.[3,5,8–10,12,15] This enables one to reach the jellification of chitosan solution, but leads to a sacrifice of one of its important advantages, being its low toxicity, distinctive biological activities and structural similarity to natural glycosaminoglycans.[11,16]

The uniqueness of chitosan, of which a macromolecule consists of primarily of β(1 → 4) linked D-glucosamine residues (Fig. 1), is also in that it is the only cationic polysaccharide. Others are anionic or noncharged. Positively charged groups make the chitosan very sensitive to the presence of anionic substances in its solutions.[13,16–18] As introduced, they associate with cationically charged macromolecules, bringing about the precipitation. The effect takes place in cases of even trace amounts of anionic substances added. It makes it impossible to jellify its solutions through the polyelectrolyte complex formation with oppositely charged polyelectrolytes. It has been demonstrated in great number of works published over the past four decades when the polysaccharide was under extensive study [13,16–29]

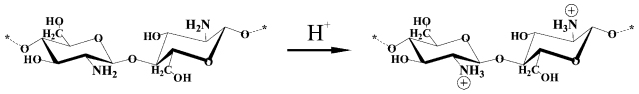

Fig. 1 Structural formulae of chitosan in charged and noncharged forms at various pH of aqueous solution. Deacetylated glucosamine residues are only shown.

Recently we have suggested a novel method to prepare chitosan hydrogels with the retention of its unique advantages, not using a chemical modification or cross-linking.[30] It is based on the ability of the amino groups to accept the proton only in a certain pH region, transferring into a charged state.[2,11,16,17] The charging results in chitosan solubilization owing to the polyelectrolyte effect. Otherwise, the chitosan is insoluble. A

[a]*Institute of Chemistry, Far East Department, Russian Academy of Sciences, 690022, Vladivostok, Russia. E-mail: YAS@ich.dvo.ru; Fax: +7 4232 348353; Tel: +7 4232 314481*
[b]*The WCU Center for Synthetic Polymer Bioconjugate Hybrid Materials, Division of Chemical Engineering, Pusan National University, San 30, Jangjun Dong, Geumjung Gu, Busan, Korea; Fax: +82 51 5137720; Tel: +82 51 510107*

† Electronic supplementary information (ESI) available: Details of the rheological measurements used to study the mechanical properties of chitosan-xanthan materials are presented. See DOI: 10.1039/b925138c

transition between the charged-nonchaged, soluble-insoluble states occurs at around pK_a value of 6.3 as shown in Fig. 1. As soon as the pH is close to or below the chitosan pK_a, the amino groups in its macromolecule accept protons that lead to the polysaccharide solubilization. If the media becomes neutral or alkaline, the polysaccharide precipitates or cannot be solubilized owing to the decrease of charging degree and transition into the noncharged state.

The dependence of charging and solubility on the pH means that the chitosan state in solutions can be regulated by adding an acid or alkali. A method suggested in [30] is based on this property, providing the jellification of chitosan solutions through *in situ* formation of polyelectrolyte complexes with anionic polysaccharides. To perform it, a solid dispersion of noncharged chitosan was dispersed first in a neutral solution of anionic polysaccharide that subsequently was acidified. The pH shift results in the polysaccharide charging (Fig. 1) that brings about two main effects. One is the solubilization of chitosan, another, its electrostatic interactions with the oppositely charged counterpart. The polyelectrolyte complex generated *in situ* provided the formation of a three-dimensional network from electrostatically associated macromolecules that led to the solution jellification.

It should be pointed out that a direct addition of acid, for example, by the dropwise did not make it possible to prepare a chitosan hydrogel. One could observe the common precipitation of its polyelectrolyte complex with anionic polysaccharides.[13,16–29,31–33] The jellification of solutions was achieved when the acidifying was carried out in a gradual manner. This was done with the help of chemical acidulating agent glucono-δ-lactone, subsequently referred to as GDL. When the GDL is brought into contact with water, it causes its hydrolysis in accordance with the reaction shown in Fig. 2. A gluconic acid thus generated results in the gradual shift of solution pH into acidic region. If there is a dispersion of chitosan in noncharged form, the acidifying results in its progressive charging. As demonstrated in our article,[30] only the gradual pH shift allowed preparing a monolithic hydrogel. Experiments were performed with the majority of industrially important anionic polysaccharides – alginate, carrageenans, carboxymethylcellulose, sodium hyaluronate and xanthan. The fact of monolithic hydrogel formation in all these cases means that the developed approach is common to the jellification of chitosan solution.

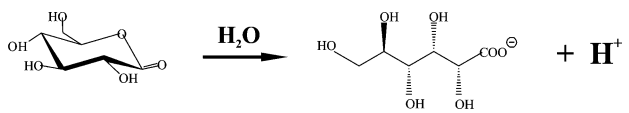

δ-Gluconolactone
(D-(+)-Gluconic acid δ-lactone)

D-Gluconic acid

Fig. 2 Structural formulae of acidulating agent glucono-δ-lactone and product of its hydrolysis generated after the hydrolysis in water.

This article is devoted to a hydrogel that is formed by chitosan with xanthan. Our study revealed a difference of this system from that of chitosan with other anionic polysaccharides. It was observed in their phase behavior and morphology. A feature of chitosan-xanthan systems is self-organization into fibrils in the course of gradual changing pH as well as, what was found for the first time, into capsules at certain charge mixing ratios of these polysaccharides. Differences from other anionic polysaccharides take also place in the mechanical properties and mechanism of jellification. Their relationship with morphology was revealed. The fibrillation was related to the unique nature of xanthan. Its macromolecules can self-assemble into a stiff double helix that makes them highly rigid.[34,35] The persistence length is longer than 100 nm.[36–39] This can be a reason for the jellification differences of chitosan with xanthan and other anionic polysaccharides. Results of detailed examination on this unique system is presented in the article.

2. Experimental

2.1. Materials

Chemical Substances. Two samples of chitosan (poly(β-(1,4)-D-glucosamine-*co*-*N*-acetyl-D-glucosamine; *ca.* 14% acetylated), xanthan and glucono-δ-lactone were purchased from Fluka. According to the supplier, the molecular weight of chitosans were *ca.* 300 kDa and *ca.* 700 kDa, xanthan, *ca.* 1000 kDa. Xanthan solutions were prepared at least 24 h before the hydrogel preparation, using distilled water. Their pH was between 6 and 7. A buffer was not added. Chitosan samples were grinded and sifted through separating sieves. A fraction of fine particles of size about 0.2 mm was separated

Preparation of hydrogels. Appropriate weighted amount of fine particles of dry chitosan was introduced and dispersed in a xanthan solution with the help of a magnetic stirrer. Thereafter a batch of GDL was added into this solution. The mixture was vigorously agitated by a magnetic stirrer to dissolve the acidulating agent and reach a homogeneous distribution of chitosan particles. After a lapse of half to few hours, which depends on the GDL and chitosan concentration, the solution viscosity was increased. This allowed stopping the stirring because the precipitation of chitosan particles was ceased. The viscosity change accelerated increasingly with time, accomplishing with a transition into a gel state. As-prepared hydrogels were monolithic. In some instances one can observe slow hydrogel shrinkage accompanied by the separating out of a solution. This phenomenon known as the syneresis could be continuing from few days to few months that depended on the polysaccharide concentrations. The syneresis S was characterized by a weight proportion of separated solution m_s to the initial weight of hydrogel m_h:

$$S = \frac{m_s}{m_h} \times 100\%$$

The phase behavior of chitosan-xanthan systems was dependable on their charge mixing ratio Z, not on the absolute concentrations. The Z value was calculated based on the charge density of each polysaccharide in accordance with the following equation:

$$Z = \frac{n_{xan} Z_{xan}}{n_{chit} Da},$$

where n_{xan} and n_{chit} are the numbers of moles of monomer residues in xanthan (Fig. 3) and chitosan (Fig. 1) macromolecules,

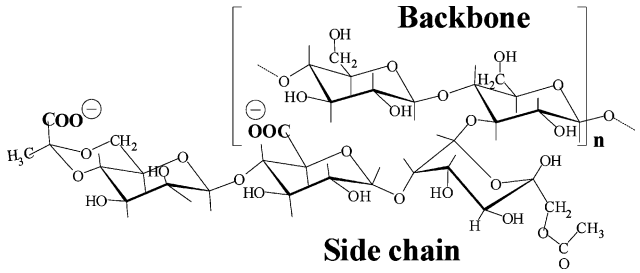

Fig. 3 Structural formula of a repeating unit in xanthan macromolecule. Charged groups are in side-chain.

respectively, z_{xan} equal to 2 is the number of charged functional groups per the monomer residue in xanthan, *Da*, the N-deacetylation degree of chitosan.

Preparation of aerogels. They served to examine the morphology under the scanning electron microscopy. Aerogels were prepared from the synthesized hydrogels after successive exchange of solvent. The water was replaced first for ethanol by soaking in a set of ethanol–water mixtures with successively increased proportion of alcohol and finally in acetone.[17] Thus prepared samples were dried by means of Critical Point Dryer 030 (Great Britain) in which acetone was initially exchanged for liquid CO_2 that then was removed at the supercritical condition.

2.2. Analytical Methods

Scanning Electron Microscopy, SEM. Examinations were performed using an EVO 40 field emission scanning electron microscope (Carl Zeiss). Aerogels were cut to have a fresh surface for observation and thereafter it was coated with platinum layer. Microscopic pictures of each sample were taken at various magnifications (150×, 400×, 1500×, 4000×, 15 000× and 40 000×) to perform a detailed examination on the morphology at various scales.

Rheological measurements. These were performed by means of a Rotovisco RT20 stress-controlled rheometer (Haake, Germany) equipped with cells that had cone-and-plate and plate-and-plate geometries. It was described in detail in ref. 40. The cone-and-plate cell was applied to study mainly mechanical properties of liquids, the plate-and-plate one, of hydrogels. The former could be used in single-gap or double-gap regimes. The cone angle was 4°, and its diameter, 60 mm. In the cell with plate-and-plate geometry the plate with diameter of 30 mm had serrated surface. Solvent evaporation in both the cells during measurements was prevented by a special chamber with a sponge soaked with water. The temperature 25 °C was controlled with an accuracy of ± 0.1 °C.

The measurements were performed in either an oscillation or creep regime. The oscillatory frequency was varied from 0.001 to 10 Hz. The frequency regime served to decide on the type of examined materials and determine the zero-shear viscosity in a case of liquids. The creep regime was used to find the zero-shear viscosity and plateau modulus for highly viscoelastic liquids and hydrogels. Further details concerning the rheological measurements may be found in the ESI.†

Dynamical Mechanical Analysis, DMA. The spectra characterizing material mechanical properties were taken by means of DMASDTA861 of Mettler-Toledo (Switzerland). Measurements were conducted in oscillatory compression regime at frequency varying in range of 0.04–10 Hz. An eight-mm bar with the thickness of 2 mm was cut from prepared chitosan-xanthan samples to place it in the holder between parallel plates. A change of linear dimension under the compression did not exceed 50 μm. The temperature was kept 25 ± 0.5 °C.

3. Results and Discussion

3.1. Hydrogel formation

The precedure was began with dispersing tiny particles of chitosan a solution of xanthan. The pH value is little over 6.3 of pK_a value of the polysaccharide. Chitosan did not swell notably and was completely insoluble in this media. Visible interactions of its dispersion with xanthan were not obvious.

A structural formula of xanthan is given in Fig. 3. This is a microbial polysaccharide produced from glucose of which molecules are (1 → 4)-linked, forming a backbone as in cellulose.[34,41] An every second residue at 0–3 position contains a covalently attached side-chain of trisaccharide composing of two mannoses and one glucuronic acid. There are 2 carboxylic groups in the side chain, whereas the backbone is noncharged. They provide negative charging of a carbohydrate macromolecule in aqueous solutions. Because only two carboxylic groups fall on five monosaccharide residues, the charge density is rather low.

The jellification was triggered by adding the GDL into a xanthan solution with dispersed chitosan. The acidulating agent causes the gradual acidification (Fig. 2). When the pH value passed and became lower than that of chitosan pK_a, the polysaccharide transforms into the charged state owing to the proton acceptance by amino groups as shown in Fig. 1. Because a charged amino group brings a positive charge, it is involved into electrostatic interactions with an oppositely charged carboxylic group in xanthan macromolecule (Fig. 3) in accordance with the following reaction:

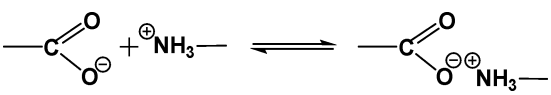

This causes the association of oppositely charged polysaccharides. Polyelectrolyte associates are commonly called the polyelectrolyte complexes.[42] The gradual pH shift and, as a result, *in situ* progressive charging of chitosan leads to a step-by-step complexation with xanthan. When performing an experiment in such the manner, one can jellify solutions (further details are given in next section).[30] Precipitation or phase separation was not observed as soon as a hydrogel was formed.

Examination of behavior of jellified solution in time revealed an appearance of syneresis. The phenomenon consists in the slow gel shrinkage accompanied with the liquid separation. This could be obvious in next day after the hydrogel preparation, continuing over the course of weeks or even months. Examination of results revealed a correlation between the amount of separated liquid and the charge mixing ratio of xanthan and chitosan in a sample. This is obvious from Fig. 4 in which corresponding experimental data are plotted against the *Z*. Each point presents a steady state achieved throughout nine months.

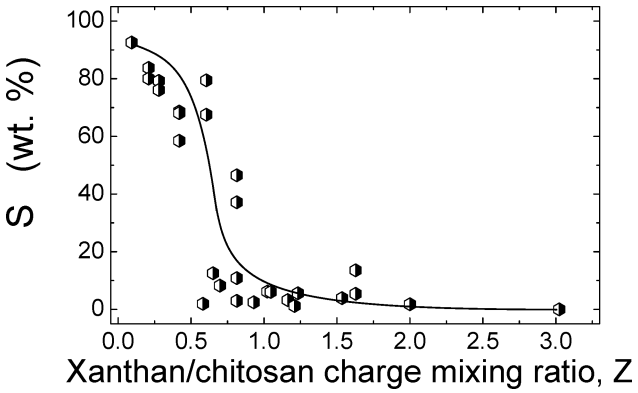

Fig. 4 Liquid phase separated owing to the hydrogel shrinkage *vs.* the charge mixing ratio Z. The observations were performed over the course of nine months to be sure of reaching the steady state.

The syneresis was generally observed when chitosan was taken in excess with respect to xanthan. When the charge mixing ratio was between 0.1–0.3, there was tremendous shrinkage of hydrogel phase. The amount of separated liquid phase could reach up to 90 wt%. A decrease of chitosan content in relation to the xanthan one resulted in a sharp drop of the separated liquid amount at Z around 0.6. This value became less than 10 wt% at $Z > 0.8$. With further increasing the charge mixing ratio of xanthan to chitosan, the amount of separated liquid did not exceed 2–3 wt% in the vicinity of $Z \sim 1.1$ and then the syneresis ceased to be visible.

The considered phase behavior of chitosan-xanthan hydrogels differs from that of systems prepared by the common mixing of solutions of oppositely charged polysaccharides. Monolithic jelly-like phases are usually formed when one of the two counterparts is taken in excess.[17,43,44] Once the charge mixing ratio is closer to 1, there is a precipitation or phase separation proceeding *via* the syneresis. Furthermore, nano-/microparticles, which were prepared by combining oppositely charged polysaccharides, were very keen to the easy flocculation in this region.[45] By the approach suggested in [30] and used here, the stable chitosan-xanthan hydrogel is progressively formed. The cationic polysaccharide is taken in noncharged form that retards the formation of polyelectrolyte complex through the fast cooperative electrostatic interactions. As soon as a unit charge appears in the course of acidification, it is involved in the local interactions. Other charged groups are generated by accident, not related with each other and spatially separated. With charging the chitosan macromolecules in such manner, the local electrostatic cross-links are progressively formed that bring about first smooth increase the viscosity and then jellification of the whole solution volume.

3.2. Mechanical properties

Xanthan, which is involved into the complexation with chitosan, can produce a hydrogel by itself. Its macromolecule adopts a 5-fold helical conformation in aqueous solutions that is stabilized by side-chains packing along the biopolymer backbone.[34–36,46,47] Two helical segments of various chains are susceptible to side-by-side association, forming a double-stranded stiff chain. This results in the occurrence of a three-dimensional network setting up solution jellification. The junctions of helical segments are tenuous. They are easily splitting under a mechanical action.[34–36,46,47] Therefore, xanthan hydrogels are weak, starting flowing as an applied stress reaching a value of the yield stress which is not high.

Fig. 5 presents a dependence of the zero-shear viscosity η_o against the polysaccharide concentration. One may see a S-shaped curve. The low-concentration region refers to a linear dependence of η_o against the xanthan concentration. This is the case of diluted solution where polymer macromolecules are isolated from each other, being in unassociated state.[48] With increasing the concentration, one can observe a deviation from the linearity. This occurs at $C_{xanthan} \geq 0.1$ wt% where is a sharp increase of the zero-shear viscosity, reaching six orders of magnitude. The deviation is evidence for the interactions between carbohydrate macromolecules. As followed from frequency dependencies of shear moduli presented in the ESI,† there is a transition from liquid-like state with Maxwell behavior to the hydrogel at $C_{xanthan}$ of about 0.5 wt%. Because the xanthan jellification is caused by the formation of double helixes by associated carbohydrate macromolecules,[34–36,46,47] the data presented in Fig. 5 point to the beginning of the association at $C_{xanthan}$ of around 0.1 wt%. Our estimation correlates well with the literature data. For instance, Harding with collaborators determined the overlapping concentration at *ca.* 0.05 wt% by using a capillary viscometer,[49] Milas *et al.*, at 0.126 wt%,[50] whereas Rodd *et al.* estimated the beginning of xanthan association from dynamic light scattering measurements at 0.07 wt%.[51]

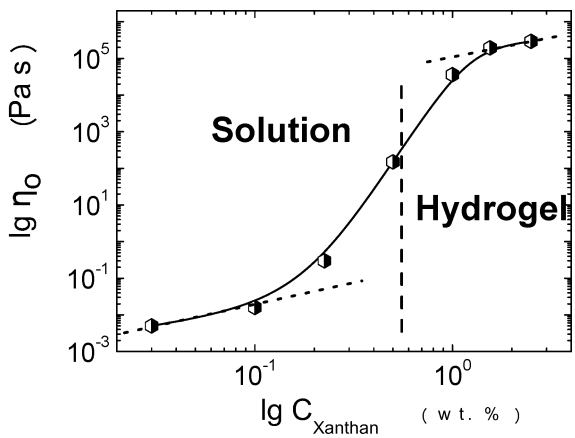

Fig. 5 The zero-shear viscosity *vs.* the concentration of xanthan in aqueous solution. The vertical dashed line shows a tentative critical concentration of polysaccharide at which a transition to the hydrogel state is observed. The measurements were performed at 25.0 ± 0.1 °C.

It is worth mentioning that the sharp increase of the zero-shear viscosity is accomplished by a gentle slopping that is close to a linear dependence. One may see it from a dotted straight line constructed as a tangent to the curve in the high concentration region. It seems that the transition to the linear slopping after the sharp rise of zero shear viscosity is suggestive of the completion of generation of three-dimensional network by associated carbohydrate macromolecules in the solution bulk. To our knowledge, this has not been analyzed in the literature yet.

The formation of a polyelectrolyte complex with chitosan influenced significantly the mechanical properties of xanthan

solution. The complexation effect is obvious from Fig. 6 in which the shaded region demonstrates a difference in the zero-shear viscosities of samples without chitosan and in its presence against the xanthan concentration. The $\Delta\eta_o$ is as much as an order of magnitude in the low-concentration region, increasing with added xanthan. Furthermore, the transition of liquid into the jellified state took place at smaller xanthan concentration. It is shown by vertical dashed lines in the plot. The rheological data in Fig. 6 evidence a much stronger three-dimensional network generation in the presence of cationic polysaccharide.

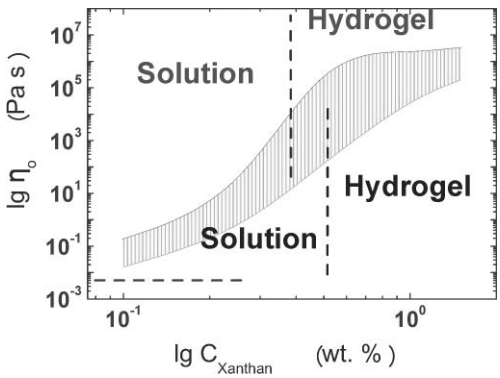

Fig. 6 The zero-shear viscosity *vs.* the concentration of xanthan in aqueous solution. The shaded area between two curves shows a difference in η_o between solutions containing only xanthan (lower curve) and xanthan with 0.5 wt% of chitosan (upper curve). The horizontal dashed line at the left bottom marks the zero-shear viscosity of 0.5 wt% chitosan solution. The vertical dashed lines represents tentative critical concentrations of polysaccharide at which a transition to the hydrogel state is observed in the absence (right line, see also Fig. 5) and presence of 0.5 wt% of chitosan (left line). Measurements were performed at 25.0 ± 0.1 °C.

Fig. 7 presents storage modulus G′ values at various charge mixing ratios of xanthan to chitosan in samples. Two regions are recognizable at a glance. A vertical dash line shows a tentative boundary between them. When $Z \geq 1.6$, the G′ slopes gently down with increasing the charge mixing ratio of oppositely charged polysaccharides. The narrower left region, where chitosan is in excess relative to the xanthan, contains a peak in the curve. The peak positions in the region in which Z values are between 0.6 and 1.0. Its maximum is at the xanthan/chitosan charge ratio of *ca.* 0.8. The sharp increase of mechanical strength in this narrow region of charge mixing ratios of polysaccharides was confirmed by additional experiments. A reason for that became obvious after a SEM study of the morphology of chitosan/xanthan hydrogels. These data are considered below.

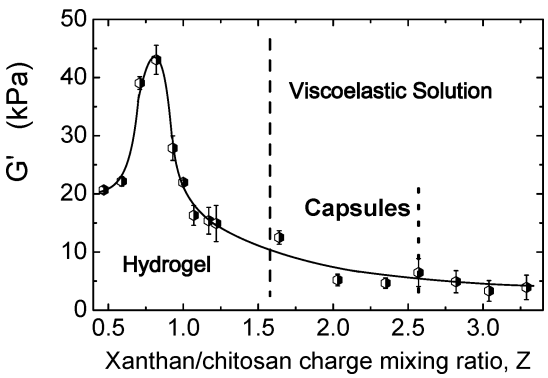

Fig. 7 The storage modulus measured at frequency of 1 Hz *vs.* the charge mixing ratio of xanthan to chitosan in the system. To perform measurements, two series of samples were independently prepared. The samples each were cut to pieces four of which were used in the measurements. Mean values are shown. The bars represent the scatter in the data. The dash line shows a tentative boundary between the hydrogel and highly viscoelastic solution, while the dot line marks the right boundary of region between two vertical lines in which capsules were found. Further details are considered in the text.

A thorough study of mechanical properties of mixtures in which xanthan is in significant excess relative to the chitosan revealed that they look like a hydrogel, but in reality there are highly viscoelastic solutions. A real hydrogel was formed where the chitosan was taken in excess and the charge mixing ratio did not exceed 1.6. The tentative boundary between these two regions are shown by vertical dash line in Fig. 7. By separating xanthan-chitosan systems into two types, we followed the suggestion of Winter and Chambon. According them, a transition from liquid to the gel state occurs at $G' \approx G''$.[52,53] A gel phase possess solid-like behavior, which is to say that storage modulus G′ is larger than the loss modulus G″. As followed from examination of frequency dependencies of shear moduli (not shown), the criterion was valid up to $Z \approx 1.6$. When mixtures with an increased charge mixing ratio of xanthan to chitosan were prepared, a viscoelastic solution was formed.

Mixtures, in which Z was varied between 1.6 and 2.6, were heterogeneous. Their examination revealed the presence of spherical capsules. Their formation is discussed in the section devoted to morphological studies.

3.3. Hydrogel morphology

The progressive charging of chitosan in a xanthan solution by the gradual acidification led first to the swelling of dispersed particles that then became more and more transparent, disappearing with time. A close examination of prepared samples by means of magnifying lens revealed heterogeneity. Its level depended on the concentrations both of chitosan and xanthan, molar ratio between them. The heterogeneity was caused by the presence of fibrillar-like structures in the hydrogel bulk. They were rather common to the chitosan-xanthan systems thus prepared. To study their morphological features, the SEM was applied. A set of pictures taken for four samples are represented in Fig. 8. They are given at three magnifications that allow gaining a more comprehensive impression about the hydrogel morphology at various length scales.

It is obvious from Fig. 8 that fibrillar-like morphology is typical of xanthan-chitosan polyelectrolyte complexes. By examining thoroughly the presented images, one can find some differences. Where the chitosan was taken in excess in relation to xanthan (Fig. 8A), rod-like particles are seen at the low magnification (upper left picture). As followed from the image made at higher magnification (bottom left picture), these particles consist of clusters of nanoparticles.

With increasing the charge mixing ratio of xanthan to chitosan in hydrogel, a transition to fibrillar-like morphology takes place (Fig. 8B–8D). Fibrils are seen at all the magnifications presented

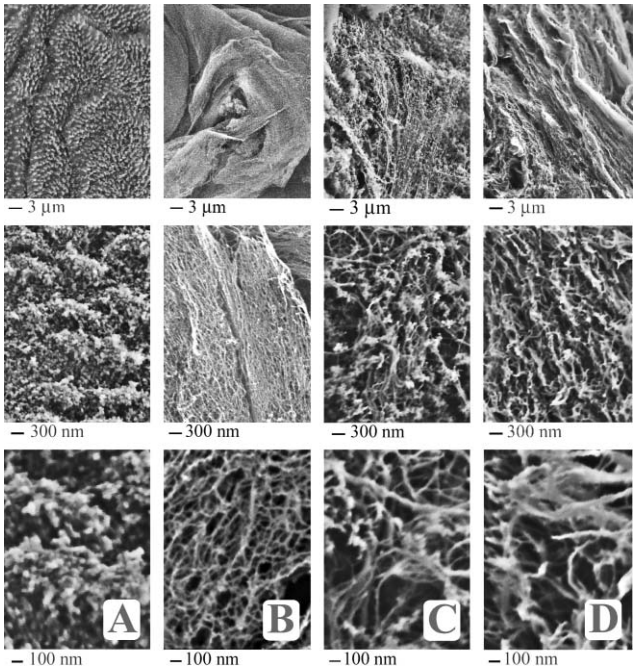

Fig. 8 SEM micrographs of aerogels prepared by the supercritical drying of initial hydrogels that were formed by xanthan and chitosan taken at charge mixing ratio of 0.47 (A), 0.8 (B), 1.0 (C) or 1.25 (D). Each sample is presented by three pictures taken at various magnifications and aligned vertically.

in Fig. 8, but there are differences between them in the thickness and alignment as charge ratio between xanthan and chitosan was varied. The thinnest fibrillar structure was formed at $Z = 0.8$ (Fig. 8B). Their diameter is mainly between 25–35 nm. It is notable that a plethora of fibrils is assembled into bundles. This is best seen at the centre image. As the charge mixing ratio of xanthan to chitosan was enhanced, the fibril diameter was increased. It is mainly varied between 40 and 50 nm at $Z = 1$ (Fig. 8C) and between 60 and 90 at $Z = 1.25$ (Fig. 8D). Furthermore, some wrinkled swelling can be seen. The fibrils are also assembled into bundles, but they are loosely packed.

It seems that it is typical of xanthan with chitosan to self-organize into fibrillar structures when they are brought into complexation. It is pertinent to mention works of Dumitriu with collaborators in this connection.[23,54,55] They prepared hydrogels by the common mixing of solutions as well as capsules by means of the dripping of one solution into another. As followed from their SEM observations, fibrillar-like morphology was found in both these cases. Of interest is that the fibril diameter varied between 50 and 100 nm. Our estimates are consistent with their result, although the preparation methods differ in significant manner.

The formation of fibrils and three-dimensional network from them (Fig. 8) accounts for the reason for the jellification of solutions when chitosan and xanthan self-organize through polyelectrolyte complex formation owing to the gradually increased electrostatic interactions. The considered variation in morphology of jellified materials means that there should be differences in their properties. We examined mechanical properties to ascertain if they correlate or not with morphological features of hydrogels. Fig. 9 presents the storage modulus values against

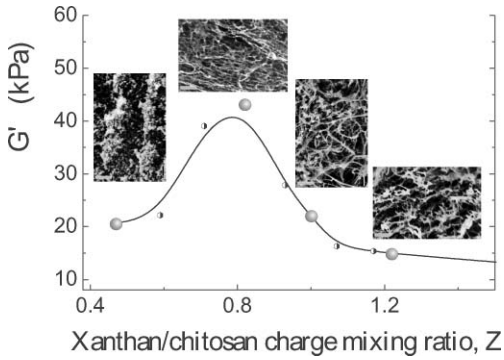

Fig. 9 The storage modulus *vs.* the charge mixing ratio of xanthan to chitosan and SEM images of aerogels corresponding the marked points in the plot at $Z = 0.47$, 0.8, 1.0 and 1.25. Further details concerning the measurements of mechanical properties and SEM observations can be found in legends, respectively, to Fig. 7 and 8. The scale bars in the pictures correspond to 500 nm.

the charge mixing ratios of xanthan to chitosan in their samples, as well as SEM images of their morphology. By examining these data, one may find that the maximum in the curve correlates with the formation of the thinnest and most tightly packed fibrils assembling into bundles. As soon as the fibrils become thicker and less dense packed, there is a notable decrease in the mechanical strength of hydrogels. This is an indication of a well-defined structure-function relationship.

An unusual phenomenon of capsulation was observed when chitosan was dispersed in excess of xanthan. The concentration region, in which it takes place, is marked off by vertical dashed lines in Fig. 7. The capsules were mechanically strong enough that allowed separating them for examination. They had a spherical or deformed shape (see Fig. 10A). Dimensions were varied with changing the charge mixing ratio of polysaccharides in samples. They could reach even few mm. When examining the separated capsules, we found that they had shell surrounding water core. The shell was mechanically strong. The solution was not leaked through it even under an applied stress. By examining it under the SEM, one may find sheet-like particles (Fig. 10B and 10C). They are closely packed at the outer surface, forming dense film. The inner side consists of randomly packed sheets that are arranged into porous structure.

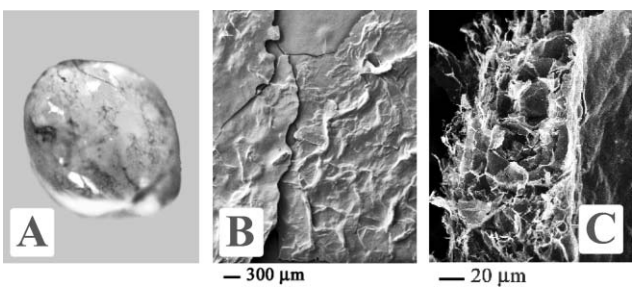

Fig. 10 Images of a capsule (A), its surface (B) and shell (C). The capsule was 1.1 mm across. It was separated from chitosan-water mixture and seen with an optical microscope (60×). The images B and C were taken with the SEM. The former presents the surface of capsule, which was dried at supercritical conditions, the latter, the shell prepared by cutting a freeze-dried capsule. It is oriented by its outer surface to the right.

A reason for the capsulation is unknown at present. Preliminary data, which are available, do not gain an insight into the mechanism of processes. Of great interest is that the self-organization of chitosan with xanthan into polyelectrolyte complex proceeds at macromolecular or nanoscopic level, whereas the capsules are microscopic objects. It seems that the controlled complexation through the gradual charging of chitosan macromolecules triggers self-regulating processes of supramolecular organization going from bottom to the up.

The capsulation and formation of unlinked nano-/miscroscopic sheets by chitosan with xanthan does not provide the generation of a three-dimensional network in the solution bulk. This makes it obvious why viscoelastic solution was found instead of the hydrogel when the charge mixing ratio exceeded 1.6 (see Fig. 7).

3.4. Mechanism of jellification

The fibrillar morphology of chitosan-xanthan hydrogels (Fig. 8), in our opinion, is evidence of spatial orientation of carbohydrate macromolecules in the polyelectrolyte complex. It is reasonable to relate it to the xanthan. This semi-flexible polysaccharide possesses a high persistence length. As determined by various authors, it runs to 30 ± 4,[37 45 56] nm or 68 ± 7,[37] 120 ± 20,[36,56] 150[38] nm when xanthan is, respectively, in the coil or helical state as double-stranded chains in solution. These data were obtained in solutions with rather high ionic strength. When it was examined in the absence of inorganic salts as in our study, the persistence length was longer, reaching 417 nm.[39] The corresponding value for chitosan macromolecule falls far short of that for xanthan. In accordance with estimations made in various works.[11,57,58] its value lies between 5 and 15 nm.

The stiff xanthan macromolecule has to be the main factor determining if there is orientation or not. The stiffness of biomacromolecules influence notably the polyelectrolyte complex formation, phase behavior and rheological properties.[17,59] The complexation of polyelectrolytes accompanied by the decrease or even elimination of charging owing to the electrostatic linkages between oppositely charged groups results in the shrinkage of macromolecular coils.[60–63] Chains with the short persistence length form compact globules that were considered as 'scrambled eggs'.[64] The stiff macromolecules self-organize into another type of polyelectrolyte complexes with a ladder-like structure.[60] The chitosan-xanthan mixture presents an intermediate case in which flexible and stiff chains are involved into the complexation. It was discussed previously in [17,59] According to the suggested model, the stiff macromolecules form a framework of three-dimensional network, while the flexible ones bearing the opposite charges serve as cross-linking junctions. Our interpretation of fibrillar morphology observed in Fig. 8 follows this model.

A set of schematic drawings in Fig. 11 concerns main stages of the self-organization of chitosan and xanthan into fibrils. The former is taken in noncharged form, the latter, in charged one (Fig. 11A). When first charged groups have appeared in different spatially separated segments which are, *e. g.*, at the opposite ends of macromolecule, they can come into electrostatic interactions with two neighboring xanthan chains being at the opposite sides.

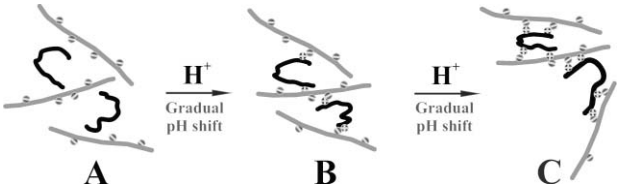

Fig. 11 A schematic representation of self-organization of oppositely charged polysaccharides in the course of progressive charging of chitosan by means of gradual acidification. A: *Initial state*. The uncharged chitosan is dispersed in solution of anionic xanthan. B: *The beginning of charging*. As-generated cationic amino groups are involved into electrostatic interactions with neighboring anionic carboxyl groups in xanthan macromolecules. C: *Self-organization of chitosan and xanthan*. The progressive charging of chitosan leads to the formation of further electrostatic linkages with time. Two cases are shown. Further details of suggested mechanism may be found in the text.

Following charged groups are generated between the first ones. Their electrostatic interactions with opposite charges in xanthan macromolecules lead to a decrease of the distance between them. Two cases are conceivable. The upper part of drawing in Fig. 11C shows the alignment of chains. This happens because the following charges in chitosan macromolecules are generated between the first ones, being shortly spaced. Linkages, which are formed between amino and carboxylic groups, are possible if xanthann macromolecules come within short distance of each other. The approaching can proceeds through alignment because of steric restrictions for the stiff xanthan chains with the high persistence length. Chitosan serves as a bridging linker between them. drawing one to another.

Another plausible case can be realized when chitosan comes into electrostatic interactions with a terminal segment of xanthan chain. This is also presented schematically in the bottom part of drawing of Fig. 11C. The approaching of the xanthan macromolecule to one another by its terminal segment can be by way of reorientation at the angle to neighboring macromolecules. When such is the case, the branching of fibrils will be generated instead of alignment.

Both the considered possibilities will lead to the self-organization of chitosan with xanthan into three-dimensional network that provide the jellification of their solution. The alignment of stiff carbohydrate macromolecules results in the fibril formation, whereas their reorientation leads to generation of branches (Fig. 11). The results concerning the hydrogel morphology in Fig. 8 make it obvious that the self-organization of chitosan and xanthan in their mixture depends notably on their molar ratio in the mixture. This opens a means to fabricate materials with various nanosized structural elements and manipulate their properties.

Chitosan hydrogels, which are prepared by the developed approach, can be applied in the same areas in which this polysaccharide is currently used. It includes biomaterials, tissue engineering, immobilization matrix and drug-delivery systems, The absence of precipitation and syneresis in some formulations provides an additional opportunity that is in loosely packed structure, whereas the fibrils make the hydrogels sufficiently strong. It was also found that the adhesiveness of these materials depends on the ratio between chitosan and xanthan in their mixture. Because of negative charges at the most surfaces,

cationic polysaccharide has an affinity for them. By varying mixture composition, one can regulate the affinity. The chitosan-xanthan ratio is of importance for the immobilization and leakage of entrapped substances. Their release is slowed down if their charge is opposite in sign to the net charge of matrix. Another important observation was that the hydrogel swelling is changed with the pH. As an acid or base is added, the charge balance between the oppositely charged polysaccharides is changed, as well as the degree of electrostatic interactions. This property is of practical consequence for drug-delivery systems. The chitosan hydrogels on the basis of self-organized polyelectrolyte complexes with anionic polysaccharides offer a fertile field for developing various types of biocompatible materials.

Conclusions

This work presents results on thorough studies of materials prepared by the gradual charging of chitosan in solution of anionic xanthan. By this manner as-appeared cationic charges are involved into step-by-step electrostatic interactions that resulted in polysaccharide self-organization into supramolecular structures through self-regulating processes of polyelectrolyte complex formation. The generation of fibrils or capsules was observed. A main factor determining the type of structural organization of interacting polysaccharides was the charge mixing ratio between xanthan and chitosan in their initial solution. The fibrillation was related to stiff macromolecules of xanthan possessing huge persistence length. Chitosan, of which macromolecules are overwhelmingly more flexible, serves as a bridging linker between stiff chains, causing their approaching and alignment. The mechanism of capsulation is presently unclear. The electrostatically interacting chitosan and xanthan could self-organize into sheet-like structures that self-close, forming a dense shell. The established fibrillation and capsulation present an interesting example of self-organization that propagates from bottom to the up, starting from the interactions between functional groups and accomplishing by the generation of nano-/microscopic structures. In our opinion, the developed method opens a fresh opportunity for the fabrication of materials with regulated structure and properties.

Acknowledgements

We thank Ms Nadya Ivanova for her help with preparations of samples for examination, Mr Vladimir Silant'ev for his assistance in the rheological measurements, Mr Denis Fomin for his technical assistance with SEM observations. This work was partially supported by research grants from the Presidium of Far East Department, Russian Academy of Sciences and World Class University Program of Ministry of Education, Science and Technology of Korea (grant R32-2008-000-10174-0).

Notes and references

1 G. A. F. Roberts, *Chitin Chemistry*, MacMillan Education, Basingstoke, Hampshire,UK, 1992.
2 E. Khor, *Curr. Opin. Solid. State. Mat. Sci.*, 2002, **6**, 313.
3 R. N. Tharanathan and F. S. Kittur, *Crit. Rev. Food Sci. Nutrition*, 2003, **43**, 61.
4 T. D. Rathke and S. M. Hudson, *J. Macromol. Sci. -Rev. Macromol. Chem. Phys.*, 1994, **C34**, 375.
5 J. G. Winterowd, P. A. Sandford, *Chitin and chitosan. In Food polysaccharides and their applications*, ed. A. M. Stephen, Marcel Dekker: New York, 1995, pp. 441–462.
6 D. K. Singh and A. R. Ray, *J. Macromol. Sci. -Rev. Macromol.*, 2000, **C40**, 69.
7 H. Ueno, T. Mori and T. Fujinaga, *Adv. Drug Delivery Rev.*, 2001, **52**, 105.
8 Y. A. Shchipunov and I. V. Postnova, *Composite Interf.*, 2009, **16**, 251.
9 J. W. Rhim, *Food Sci. Biotechnol.*, 2006, **15**, 925.
10 E. V. Shumilina and Yu. A. Shchipunov, *Colloid J.*, 2002, **64**, 372.
11 M. Rinaudo, *Prog. Polym. Sci.*, 2006, **31**, 603.
12 Yu. A. Shchipunov, *J. Colloid Interface Sci.*, 2003, **268**, 68.
13 H. Yi, L. Q. Wu, W. E. Bentley, R. Ghodssi, G. W. Rubloff, J. N. Culver and G. F. Payne, *Biomacromolecules*, 2005, **6**, 2881.
14 K. Y. Lee and D. J. Mooney, *Chem. Rev.*, 2001, **101**, 1869.
15 W. Arguelles-Monal, F. M. Goycoolea, C. Peniche and I. Higuera-Ciapara, *Polym. Gels Networks*, 1998, **6**, 429.
16 J. Berger, M. Reist, J. M. Mayer, O. Felt and R. Gurny, *Eur. J. Pharm. Biopharm.*, 2004, **57**, 35.
17 Y. A. Shchipunov and I. V. Postnova, *Composite Interf*, 2009, **16**, 251.
18 A. Drogoz, L. David, C. Rochas, A. Domard and T. Delair, *Langmuir*, 2007, **23**, 10950.
19 Y. Kikuchi and A. Noda, *J. Appl. Polym. Sci.*, 1976, **20**, 2561.
20 H. Fukuda and Y. Kikuchi, *Macromol. Chem.*, 1977, **178**, 2895.
21 W. Anguelles-Monal, M. GaHrciga and C. Peniche-Covas, *Polymer Bulletin*, 1990, **23**, 307.
22 H. Tomida, C. Nakamura and S. Kiryu, *Chem. Pharm. Bull. Tokyo*, 1994, **42**, 979.
23 S. Dumitriu, P. Magny, D. Montane, P. F. Vidal and E. Chornet, *J. Bioact. Compatible Polym.*, 1994, **9**, 184–209.
24 A. Denuziere, D. Ferrier and A. Domard, *Carbohyd. Polym.*, 1996, **29**, 317.
25 A. Hugerth, N. Caramlelham and L. O. Sundelof, *Carbohyd. Polym.*, 1997, **34**, 149.
26 H.-J. Kim, H.-C. Lee, J.-S. Oh, B.-A. Shin, C.-S. Oh, R.-D. Park, K.-S. Yang and C.-S. Cho, *J. Biomater. Sci. Polymer edn*, 1999, **10**, 543.
27 T. Sakiyama, H. Takata, M. Kikuchi and K. Nakanishi, *J. Appl. Polym. Sci.*, 1999, **73**, 2227.
28 L. Rusu-Balaita, J. Desbrieres and M. Rinaudo, *Polym. Bull.*, 2003, **50**, 91.
29 L. Bourdillon and C. Wandrey, *Colloid Polym. Sci.*, 2004, **282**, 1247.
30 Y. A. Shchipunov, N. A. Ivanova and S. A. Sarin, *Mendeleev. Commun.*, 2009, **19**, 149.
31 C. A. McKnight, A. Ku, M. F. A. Goosen and D. Sun, *C. J. Bioactive Compatible Polym.*, 1988, **3**, 334.
32 A. Bartkowiak and D. Hunkeler, *Colloid. Surf. B.*, 2001, **21**, 285.
33 T. Mitsumata, Y. Suemitsu, K. Fujii, T. Fujii, T. Taniguchi and K. Koyama, *Polymer*, 2003, **44**, 7103.
34 I. W. Cottrell, K. S. Kang, P. Kovacs, *Xanthan gum. In Handbook of Water-Soluble Gums and Resins*, ed. R. L. Davidson, McGram-Hill Book Company: New York, 1980, pp. 24–31.
35 V. J. Morris, *Science, Structure and Applications of Microbial Polysaccharides In Gums and Stabilisers for the Food Industry 5*, ed. G. O. Phillips, P. A. Williams, D. J. Wedlock, IRL Press: Oxford, 1990, pp. 315–328.
36 T. Sato, T. Norisuye and H. Fujita, *Macromolecules*, 1984, **17**(12), 2696–2700.
37 B. T. Stokke and D. A. Brant, *Biopolymers*, 1990, **30**, 1161.
38 G. Berth, H. Dautzenberg, B. E. Christensen, S. E. Harding, G. Rother and O. Smidsrod, *Macromolecules*, 1996, **29**, 3491.
39 T. A. Camesano and K. J. Wilkinson, *Biomacromolecules*, 2001, **2**, 1184.
40 Y. A. Shchipunov, *J. Colloid Interface Sci.*, 2003, **268**, 68.
41 F. Garcia-Ochoa, V. E. Santosa, J. A. Casas and F. Gomez, *Biotechn. Adv.*, 2000, **18**, 549.
42 H. Dautzenberg, W. Jaeger, J. Kotz, B. Philipp, C. Seidel, *Polyelectrolytes: Formation, Characterization and Applications*, Hanser: Munich, 1994.
43 Y. A. Shchipunov and I. V. Postnova, *Russ. J. Phys. Chem.*, 2001, **75**, 1795.

44 Y. A. Shchipunov, O. G. Mukhaneva, N. M. Shevchenko and T. N. Zvyagintseva, *Polym. Sci. Ser A.*, 2003, **45**, 295.
45 S. Boddohi, N. Moore, P. A. Johnson and M. J. Kipper, *Biomacromolecules*, 2009, **10**, 1402.
46 E. R. Morris and I. T. Norton, *Stud. Phys. Theor. Chem.*, 1983, **26**, 549.
47 S. B. Ross-Murphy, V. J. Morris and E. R. Morris, *Faraday. Symp. Chem. Soc.*, 1983, **18**, 115.
48 J. D. Ferry, *Viscoelastic Properties of Polymers*, John Wiley: New York, 1980.
49 R. Dhami, S. E. Harding, T. Jones, T. Hughes, J. R. Mitchell and K. M. To, *Carbohyd. Polym.*, 1995, **27**, 93.
50 M. Milas, M. Rinaudo, M. Knipper and J. L. Schuppsier, *Macromolecules*, 1990, **23**, 2506.
51 A. B. Rodd, D. E. Dunstan and D. V. Boger, *Carbohyd. Polym.*, 2000, **42**, 159.
52 H. H. Winter and F. Chambon, *J. Rheol.*, 1986, **30**, 367.
53 F. Chambon and H. H. Winter, *J. Rheol.*, 1987, **31**, 683.
54 F. Chellat, M. Tabrizian, S. Dumitriu, E. Chornet, P. Magny, C. H. Rivard and L. Yahia, *J. Biomed. Mater. Res.*, 2000, **51**, 107.
55 S. Dumitriu and E. Chornet, *Adv. Drug Delivery Rev.*, 1998, **31**, 223.
56 M. Rinaudo, *Food Hydrocolloids*, 2001, **15**, 433.
57 J. Brugnerotto, J. Desbrieres, L. Heux, K. Mazeau and M. Rinaudo, *Macromol. Symp.*, 2001, **168**, 1.
58 C. Schatz, J. M. Lucas, C. Viton, A. Domard, C. Pichot and T. Delair, *Langmuir*, 2004, **20**, 7766.
59 Y. A. Shchipunov and I. V. Postnova, *Polym. Sci. Ser A.*, 2006, **48**, 171.
60 A. B. Zezin and V. A. Kabanov, *Russ. Chem. Rev.*, 1982, **51**, 1447.
61 A. B. Zezin, V. A. Izumrudov and V. A. Kabanov, *Macromol. Symp.*, 1996, **106**, 397.
62 B. Philipp, H. Dautzenberg, K. J. Linow, J. Kotz and W. Dawydoff, *Prog. Polym. Sci.*, 1989, **14**, 91.
63 E. Tsuchida and K. Abe, *Adv. Polym. Sci.*, 1982, **45**, 1.
64 H. Dautzenberg, J. Hartmann, S. Grunewald and F. Brand, *Ber. Bunsenges. Phys. Chem. Chem. Phys.*, 1996, **100**, 1024.